Rev. Mexicana Astron. Astrof., **25**, 95-101 (1993)

A COMPARISON BETWEEN ANALYTIC AND NUMERICAL RESULTS OF A STEADY JET MODEL

S. Biro [1,2], J. Cantó[1], A.C. Raga[2,3], and L. Binette[4]

Received 1993 January 11

RESUMEN

Las estructuras de nudos o condensaciones compactas bien alineadas en chorros estelares pueden interpretarse en términos de modelos de choques internos cruzados. En este trabajo se presentan nuevos modelos analíticos y numéricos para la formación de choques cruzados en chorros estacionarios. Se encuentra un buen acuerdo entre los modelos analíticos y numéricos lo cual permite hacer predicciones concretas sobre las propiedades de los choques cruzados en función de los parámetros del flujo. Estas predicciones son importantes al tratar de identificar las estructuras de choques cruzados que posiblemente existen en los chorros estelares.

ABSTRACT

The structures of well aligned knots in stellar jets can be interpreted in terms of crossing shock models. In this paper, new analytic and numerical models for the formation of crossing shocks in steady jets are presented. The good agreement found between the analytic and numerical results allows us to present clear predictions of the properties of steady crossing shocks as a function of the flow parameters. These predictions should be useful for trying to identify the crossing shock structures that possibly exist in stellar jets.

Key words: **HYDRODYNAMICS — ISM – JETS AND OUTFLOWS — SHOCK WAVES**

1. INTRODUCTION

The subclass of Herbig-Haro (HH) objects called stellar jets have an emission line spectrum typical of the cooling regions of shock waves with velocities $\sim$ 20 to 100 km s^{-1}. At this time, it is not quite clear what mechanism produces these shocks. The following different scenarios have been proposed for the formation of the chains of knots observed in stellar jets:

a) Instabilities at the outer boundaries of jets can give rise to the formation of internal shocks, which might correspond to the observed knot structures. In the context of stellar jets this possibility has been studied analytically by Bührke, Mundt, & Ray (1988) and by Silvestro et al. (1987), and numerically by Blondin, Fryxell, & Königl (1990).

b) A time-variability in the ejection velocity can result in the formation of "internal working surfaces", which might correspond to the observed knots (Raga et al. 1990*b*; Kofman & Raga 1992).

c) Jets with an initial pressure imbalance with the surrounding medium develop a chain of steady internal crossing shocks. The properties of such flows (in the context of stellar jets) have been studied analytically by Cantó, Raga, & Binette (1989) (hereafter Paper I) and numerically by Falle, Innes, & Wilson (1987) and Raga, Binette, & Cantó (1990*a*).

This paper is concerned with the last of the scenarios discussed above. Throughout this paper, we will assume that the jet flow is steady, inviscid, initially underexpanded ($P_{jet} \gg P_{ext}$), cylindrically symmetrical and with solar atomic abundances (see Raga et al. 1990*a*). In the past, this flow has been studied both analytically (Paper I) and numerically (Raga et al. 1990*a*). The flow is found to develop a series of oblique, incident and reflected shock pairs as the gas in the jet expands and contracts in an effort to balance its pressure with that of the surrounding medium. These "crossing shock cells"

[1] Instituto de Astronomía, Universidad Nacional Autónoma de México.
[2] Astronomy Department, University of Manchester, U.K.
[3] Mathematics Department, UMIST, U.K.
[4] Canadian Institute for Theoretical Astrophysics.

are found to be equally spaced, and to have an approximately constant shock velocity.

In this paper, we present a detailed comparison between analytic and numerical steady crossing shock models. The differences found between these two approaches suggest possible improvements that can be made in the simplified, analytic approach. We find that these improvements in the analytic model to a large extent remove the differences between the analytic and numerical results.

2. A COMPARISON BETWEEN THE NUMERICAL AND ANALYTIC SOLUTIONS

In Paper I expressions for the value of the characteristic distances and angles of the first crossing shock cell (see Figure 1) are derived. This is done under the assumption that a narrow, highly underexpanded, highly supersonic flow with an initial radius equal to zero is injected into a medium with uniform density. The flow is assumed to have cylindrical symmetry. The jet first undergoes a Prandtl-Meyer lateral expansion, resulting in a conical flow of half opening angle α. This sudden lateral expansion causes a rapid decrease in the pressure of the gas in the jet. At the point where the jet pressure falls below the external medium pressure, the jet starts to become reconfined by the stronger external pressure by means of a shock (see Figure 1). The locus of this shock is obtained from the condition of pressure balance:

$$P_c + \epsilon_I \rho_j V_{jn}^2 = P_{ext}, \tag{1}$$

where P_c is the centrifugal pressure, $\epsilon_I = 2/(\gamma + 1)$ is a parameter of order unity (with γ the specific heat ratio), ρ_j is the jet density just before the shock

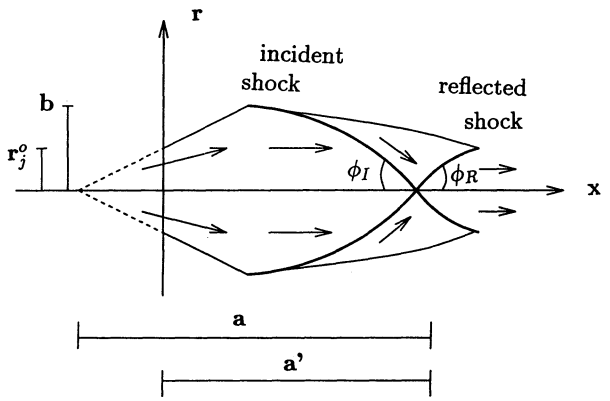

Fig. 1. Schematic djagram of the first crossing shock cell. It is shown how the flow is given an initial radius (see § 3) in the analytic solution by moving the origin of the coordinate system in the positive direction along the x-axis.

and V_{jn} is the component of the jet velocity normal to the shock. In Paper I it is assumed that $P_c \ll \epsilon_I \rho_j V_{jn}^2$, and the effect of the centrifugal pressure is thus neglected.

Solving the reduced form (with $P_c = 0$) of equation (1) it is found that the shape of the incident shock is an arc of circumference passing through the origin and crossing the symmetry axis again at:

$$a \simeq \lambda \left(\frac{\dot{M}_j V_j^o}{\pi P_{ext}} \right)^{1/2}, \tag{2}$$

where λ is a parameter of order unity which depends weakly on P_j/P_{ext}; $\dot{M}_j$ is the mass flux of the jet; V_j^o is the initial jet velocity and P_{ext} is the pressure in the external medium. The maximum separation between the symmetry axis and the incident shock is:

$$b = \frac{1}{2}(1 - cos\phi_I), \tag{3}$$

where ϕ_I is the angle formed between the incident shock and the symmetry axis. Assuming that in the initial expansion the outer layer of the jet expands laterally with constant velocity:

$$U_m = \frac{2(1-\kappa)\, c_j^o}{(\gamma - 1)}, \tag{4}$$

with c_j^o the jet gas sound speed, and:

$$\kappa \equiv \left(\frac{P_{ext}}{P_j^o} \right)^{(\gamma-1)/2\gamma}, \tag{5}$$

the initial opening angle of the jet is:

$$\sin\alpha = \frac{U_m}{V_j^o}. \tag{6}$$

We then obtain that:

$$\phi_I = \alpha + \sin^{-1}\left[\frac{1}{(\gamma\epsilon_I)^{1/2}} \frac{\kappa}{M_j{}^o} \right], \tag{7}$$

is the angle formed between the incident shock and the axis of symmetry, and that:

$$\phi_R \simeq \frac{\phi_I}{4}, \tag{8}$$

is the angle formed between the reflecting shock and the axis of symmetry (see Figure 1). Note that the expressions for the distances a and b (equations (2) and (3)) are normalized to the radius

$$R_o = [\epsilon_I \dot{M}_j V_j^o / 2\pi (1-\cos\alpha) P_{ext}]^{1/2}.$$

The value of the shock velocities associated with both the incident and reflected shocks are also predicted. They are found to be similar, and constant:

$$V_{SI} \sim V_{SR} \sim 18.7 \text{ km s}^{-1} . \quad (9)$$

for an initial jet temperature of 10^4 K.

Predictions of these parameters can also be obtained from numerical solutions of the steady crossing shock problem (see, e.g., Raga et al. 1990*a*; Raga 1989). We will carry out a comparison of the parameters of the first crossing shock cell predicted by the analytic and numerical models.

In Figure 2 we show the structure of the flow passing through the first pair of crossing shocks, which has been derived from a numerical integration of the steady flow equations. The gas is injected at $x = 0$ and flows along the x-axis. The dotted lines show 5 streamlines of the flow, and the continuous lines are isobaric contours. The loci of the shocks correspond to the regions of "piled up" pressure contours. In this figure the variables: α, a, b, ϕ_I and ϕ_R are the same as those defined above. The shock velocities (V_{SI} and V_{SR}) are calculated as the velocity of the pre-shock flow perpendicular to the corresponding shock.

In order to make a comparison between the analytic and numerical models, we define a "standard jet", with physical parameters appropriate for stellar jets (see, e.g., the observational compilation of Mundt, Brugel, & Bührke 1987). These parameters are the following: $r_j^o = 10^{16}$ cm (initial jet radius), $n_j^o = 10^4$ cm^{-3} (initial jet hydrogen number

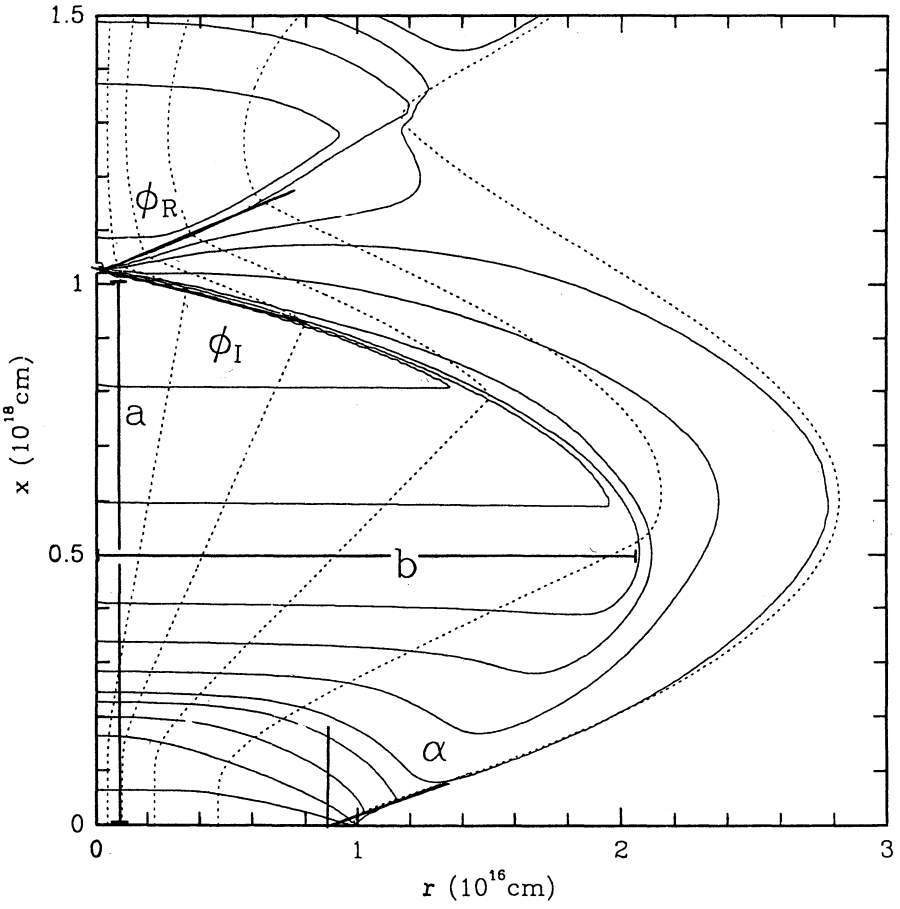

Fig. 2. Variables of the flow in the first crossing shock cell. The dotted lines show the loci of 5 streamlines. The continuous lines are isobaric contours. Characteristic lengths (a, b) and angles (α, ϕ_I, and ϕ_R) are shown. Two successive contours correspond to a pressure ratio of 2.

density), $V_j^o = 150$ km s^{-1} (initial jet velocity) and $T_j^o = 10^4$ K (initial jet temperature). The initial ionization fraction of the gas in the jet $(n_H^+/n_H)^o$ is calculated assuming coronal ionization equilibrium at the initial temperature. Our numerical model of the steady jet flow includes a self-consistent calculation of the non-equilibrium ionization state and radiative cooling rate of the gas (see Raga et al. 1990*a*, and Biro 1991).

With these initial parameters, the values for the variables a, b, α, ϕ_I, ϕ_R, V_{SI} and V_{SR} were computed from the analytic expressions, and also measured from the graphic output of the numerical code. Note that the final expressions for the distances a and b (equations (2) and (3)) are normalized to the radius R_o so the comparison is actually made with the dimensional values $a \times R_o$ and $b \times R_o$ obtained from the analytical model. The flow variables were calculated for several different values of the initial jet to external medium pressure ratio ($P_j^o/P_{ext} = 2.5$, 5, 7.5, 10, 15 and 20).

Figure 3 shows a comparison of the values obtained for the parameters a, b, α, ϕ_I and ϕ_R (see above and Figure 2) from the analytic and numerical solutions. The shock velocities were found to be independent of the initial pressure ratio. From the numerical solution, $V_{SI} = 12.3$ km s^{-1} and $V_{SR} = 16.88$ km s^{-1}, while from the analytic solution we obtain $V_{SI} \sim V_{SR} \sim 18.7$ km s^{-1} (Paper I). For most of the flow variables we find a good agreement between the values predicted by the numerical and analytic solutions. However, we find

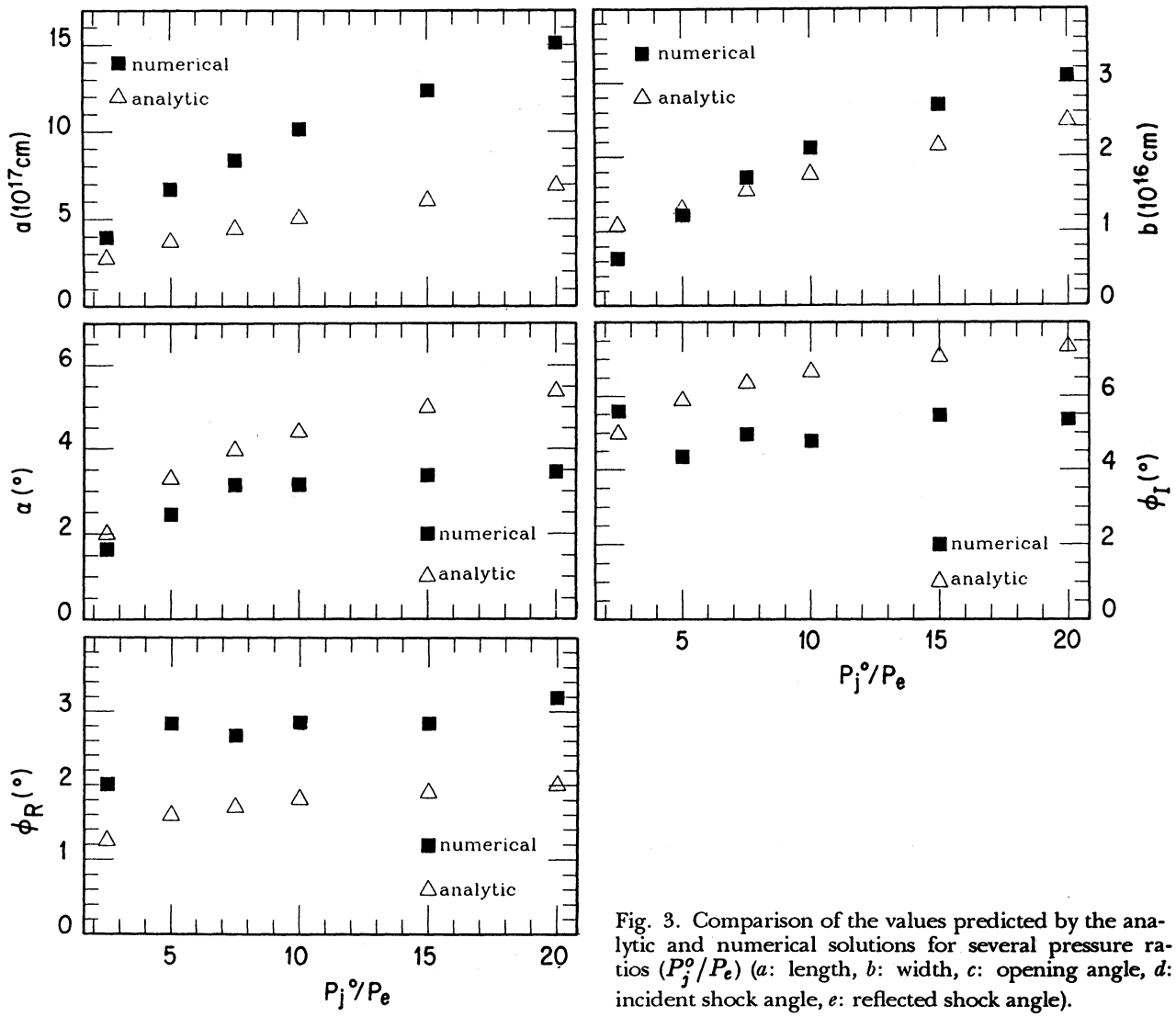

Fig. 3. Comparison of the values predicted by the analytic and numerical solutions for several pressure ratios (P_j^o/P_e) (a: length, b: width, c: opening angle, d: incident shock angle, e: reflected shock angle).

that for the distance from the point of injection to the point of reflection, a (see Figures 1 and 2), the values obtained from the numerical solution are approximately twice those obtained from the analytic solution. It can also be noted that, given the values obtained for ϕ_I and ϕ_R the ratio ϕ_I/ϕ_R differs noticeably between the analytic and the numerical solutions. The following section describes improvements to the analytic solution that partially eliminate these differences between the analytic and numerical results.

3. THE CORRECTED ANALYTIC SOLUTION

In this section, three of the assumptions which were initially made in the analytic solution are relaxed in order to obtain more accurate results.

The analytic solution described in Paper I (and briefly in § 2) is derived under the assumption that the initial jet radius is zero. A better approximation is achieved supposing a non-zero initial radius for the flow.

The approximation of a negligible initial radius for the jet can straightforwardly be removed. Changing none of the previous assumptions about the flow, but displacing the origin of coordinates in the positive direction of the x-axis (into the flow, see Figure 1), at $x = 0$ the jet will now have a non-zero radius (r_j^o). The (normalized) distance that the origin must be displaced is determined by the initial radius desired, and the opening angle of the flow (α) as follows:

$$\Delta x = \frac{r_j^o}{R_o \tan\alpha} \ , \tag{10}$$

where α is the opening angle which results from the lateral (Prandtl-Meyer) expansion of the jet gas (see equation (4)). The expression for R_o given in the previous section is used, taking the mass flux $\dot{M}_j$ at the distance Δx to be:

$$\dot{M}_j = 2\pi\rho_j^o V_j^o \Delta x^2 \ \frac{1-\cos\alpha}{\cos\alpha}. \tag{11}$$

The resulting displacement is:

$$\Delta x = \frac{\kappa^{\gamma/(\gamma-1)}\ (\cos\alpha)^{1/2}}{(2-\epsilon_I)^{1/2}\ M_j^o} \ , \tag{12}$$

which implies a new characteristic length a' of the form:

$$a' = a - \Delta x \ . \tag{13}$$

Another assumption used to derive the analytic solution of Paper I is that the centrifugal pressure P_c (which appears in a gas flowing along a curved trajectory) is much smaller than the jet's ram pressure P_{ram} (normal to the shock) and the external medium's thermal pressure P_{ext}, and can thus be ignored. Very near the point where the shock front is reflected, we find that this is not true, so that this centrifugal pressure must be included in the pressure balance equation which is used to calculate the locus of the incident shock. The complete form of the pressure balance equation (1) is now used, and (unlike the previous $P_c = 0$ case) the solution to this equation is a complex integro-differential equation for the locus of the incident shock $r(\theta)$:

$$\frac{1}{(r^2+r'^2)} - (1-\epsilon_I)\left(\frac{r_*}{r}\right)^{2\gamma} +$$

$$+\frac{1}{\epsilon_I}\left(\frac{r^2+2r'^2-rr'}{(r^2+r'^2)^{3/2}}\right)\frac{1}{r\cos\theta}$$

$$\int_{\theta_*}^{\theta} \frac{r'}{(r^2+r'^2)^{1/2}} \cos\theta\, d\theta = 1 \ , \tag{14}$$

where r is the radius in units of r_* (the radius at which the jet pressure equals the ambient pressure) and r' is the derivative of the radius with respect to θ. The solution of this equation (which has been described in detail by Cantó 1980) gives the shape and size of the incident shock, from which a more precise value for the length a can be obtained.

Both of these corrections can be combined to calculate a new value for the length a. The values obtained from the solution of equation 14 can then be corrected for the effect of a non-zero initial radius using equation 13, thus obtaining a value of a which contains both of the corrections to the analytic theory that have been described above. These results are compared to the numerical values in Figure 4. This plot shows that these corrections to the analytic theory result in a good agreement between the values of a predicted from the analytic and numerical models.

We find that the assumption that the reflected (second) shock is strong is probably the cause for the difference between the analytic and numerical ϕ_I/ϕ_R ratios (see § 2 and Figures 3*d* and 3*e*). Although for high P_j^o/P_{ext} values the incident shock is indeed strong, this is not the case for the reflected shock. We have removed this assumption, and we now consider the full jump conditions (rather than the strong shock limit) across the reflected shock. Combining the equations for the normal and

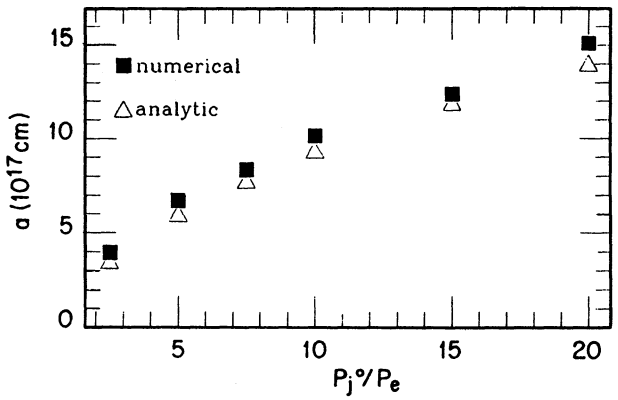

Fig. 4. Comparison of the value of a predicted by the corrected analytic and the numerical solutions.

tangential velocity jumps across the first and second shock, we obtain the following expressions:

$$\tan\beta = \xi_I \tan\phi_I, \tag{15}$$

$$\tan\phi_R = \xi_R \tan(\phi_I + \phi_R - \beta), \tag{16}$$

where ϕ_I and ϕ_R are the angles that the incident and reflected shocks form with the symmetry axis, β is the angle between the shock front and the flow direction just after the incident shock and ξ_I and ξ_R are the inverse of the compression factors across each shock. Because the incident shock is strong, $\xi_I = 1/4$ (for $\gamma = 5/3$). ξ_R depends on the Mach number of the flow and γ as follows:

$$\xi_R = \frac{(\gamma-1)M_R^2 + 2}{(\gamma+1)M_R^2}, \tag{17}$$

with the Mach number of the flow normal to the shock:

$$M_R = \frac{V_j \sin(\phi_I + \phi_r - \beta)}{c_R}, \tag{18}$$

where c_R is the sound speed just before the reflected shock:

$$c_R = c_1\left(\frac{\rho_R}{\rho_1}\right)^{(p-1)/2}, \tag{19}$$

with c_1 the sound speed just behind the incident shock. ρ_R/ρ_1 is the density change from the exit of the incident shock to just before entering the reflected shock. The density rises simply because the jet flow is directed towards the symmetry axis by the incident shock, and the cross section of the jet is reduced. This density jump is:

$$\frac{\rho_R}{\rho_1} = \frac{\sin(\phi_I + \phi_R - \beta)}{\sin\beta}\frac{\sin\phi_I}{\sin\phi_R}. \tag{20}$$

Finally, p is a polytropic index such that, if the gas is adiabatic, $p = 5/3$ and if it is isothermal, $p = 1$. Assuming that the angles are small, equations 15, 16 and 20 can be simplified and we obtain an expression for the shock angle ratio as follows:

$$\frac{\phi_I}{\phi_R} = \frac{4}{3} - \frac{(1-\xi_R)}{\xi_R}. \tag{21}$$

Assuming that the gas is monotonic and that the flow is adiabatic, from equation 21 we obtain that $\phi_I/\phi_R = 1.06$. If the flow is isothermal, we obtain a ratio of $\phi_I/\phi_R = 2$. Figure 5 shows these analytic results plotted as a function of the pressure ratio P_j^o/P_{ext} for both the adiabatic and isothermal limits. Also plotted are the values measured from the numerical solution. We find that the adiabatic and isothermal values of ϕ_I/ϕ_R bracket the results obtained from the numerical models. This is consistent with the fact that our numerical models are nonadiabatic (see § 2).

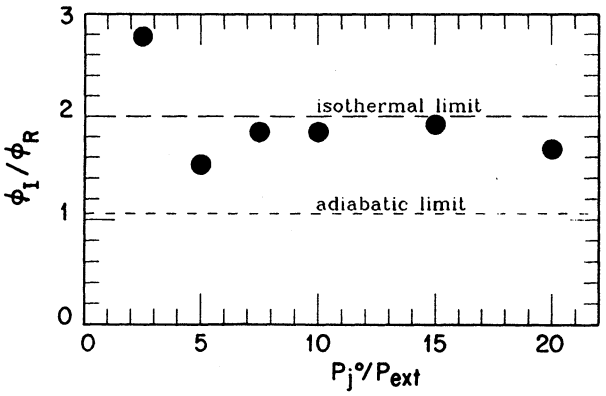

Fig. 5. Shock angle ratio (ϕ_I/ϕ_R) versus initial pressure ratio (P_j^o/P_{ext}). The points are the values measured from the non-adiabatic numerical model. The lines are the values calculated with the corrected analytic solution (the isothermal and adiabatic limits are shown).

4. DISCUSSION

A comparison has been made between the analytic and numerical solutions of a steady jet model. The values predicted from these two solutions for

the variables b, α, ϕ_I, ϕ_R, V_{SI} and V_{SR} (for the flow in the first crossing shock pair) show a reasonably good agreement. We find that the shock velocity is approximately the same for both the incident and the reflected shocks, and the value obtained ($V_S \sim 15$ km s^{-1}) is similar for both solutions. Such low shock velocities appear to be in qualitative agreement with observations of stellar jets, which show very low excitation emission line spectra (see, e.g., Raga et al. 1990*a*).

The values of the characteristic length a of the first crossing shock cell and the ratio ϕ_I/ϕ_R between the angles of the incident and reflected shocks predicted by the original analytic theory of Paper I do not agree well with the values obtained from the numerical model. Because of this disagreement, we have derived a revised analytic solution.

In particular, we have removed the assumption of a negligible initial jet radius, and we have included a centrifugal pressure term in our equation (which had been neglected in Paper I). We also have considered the full jump conditions for the reflected shock (in the original analytic solution it had been assumed that the reflected shock is strong). A new analytic value is then obtained for a, which compares quite well with the numerical value. Analytic limits are obtained for the ratio ϕ_I/ϕ_R for the adiabatic and isothermal cases, and it is found that the numerical predictions for a non-adiabatic flow fall between these values of the ϕ_I/ϕ_R ratio.

Therefore, we now have a coherent analytic and numerical model for the formation of steady crossing shocks in stellar jets. The general predictions of this model are that the jet will present oblique ($\phi_I \sim 5^o$ and $\phi_R \sim 2^o$) internal crossing shocks with low shock velocities ($V_S \sim 15$ km s^{-1}). The mechanism for the formation of these shocks, as well as analytic and numerical predictions of the observable parameters (e.g., the shock velocities and the lengths of the crossing shock cells) now appear to be well understood and on a firm theoretical footing.

The authors would like to thank J. Dyson and J. Arthur for reviewing this manuscript. We are also grateful to the referee for the suggestions to better the text. S.B. wishes to acknowledge support from DGAPA-UNAM (México), ORS and Manchester University.

REFERENCES

Biro, S. 1991, B.Sc. Thesis (Universidad Nacional Autónoma de México)
Blondin, J.M., Fryxell, B.A., & Königl, A. 1990, ApJ, 360, 370
Bürhke T., Mundt, R., & Ray, T.P. 1988, A&A, 200, 99
Cantó, J. 1980, A&, 86, 327
Cantó, J., Raga, A.C., & Binette, L. 1989, RevMexAA, 17, 65 (Paper I)
Falle, S.A.E.G., Innes, D.E., & Wilson, M.J. 1987, MNRAS, 225, 741
Kofman, L., & Raga, A.C. 1992, ApJ, 390, 359
Mundt, R., Brugel, E.W., & Bürhke, T. 1987, ApJ, 319, 275
Raga, A.C. 1989, in Proc. of the ESO Low Mass Star Formation and Pre-Main Sequence Objects, ed. B. Reipurth (Garching: ESO), p. 281
Raga, A.C., Binette, L., & Cantó, J. 1990*a*, ApJ, 360, 612
Raga, A.C., Cantó J., Binette, L., & Calvet, N. 1990*b*, ApJ, 364, 601
Silvestro, G., Ferrari, A., Rosner, R., Trusonni, E., & Tsinganos, K. 1987, Nature, 325, 228

Luc Binette: Canadian Institute for Theoretical Astrophysics, 60 St. George Street, Toronto, Ontario, M5S 1A1, Canada.
Susana Biro: Astronomy Department, University of Manchester, Manchester M13 9PL, U.K.
Jorge Cantó: Instituto de Astronomía, UNAM, Apartado Postal 70-264, 04510 México, D.F., México.
Alejandro C. Raga: Mathematics Department, UMIST, P.O. Box 88, Manchester M60 1QD, U.K.